Structural Changes of Mo/ZSM-5 Catalysts During the Methane Dehydroaromatization

Z.R. Ismagilov[1a*], E.V. Matus[a], I.Z. Ismagilov[a], M.A. Kerzhentsev[a], V.I. Zailovskii[a], K.D. Dosumov[b], A.G. Mustafin[c]

[a] Boreskov Institute of Catalysis, Novosibirsk, Russia
[b] JCS "D.Sokolski Institute of Organic Catalysis and Electrochemistry", Almaty, Kazakhstan,
[c] Bashkir State University, Ufa, Russia

Abstract

The structure changes of Mo/ZSM-5 catalysts with different Mo content (2 and 10 wt. % Mo) and Si/Al atomic ratio (17, 30 and 45) during the methane dehydroaromatization have been investigated by X-ray powder diffractometry, N_2 adsorption and transmission electron microscopy. The treatment of Mo/ZSM-5 catalysts in reducing atmosphere (CH_4 or H_2) at about 700°C promotes development of mesoporous system. The pores are open to the exterior of the zeolite grain and have an entrance diameter of ~ 4-10 nm. It is proposed that mesopore formation in Mo/ZSM-5 catalyst is connected with the dealumination of zeolite. The mesopore formation in the parent H-ZSM-5 zeolite by NaOH treatment does not improve the activity of Mo/ZSM-5 catalyst.

Introduction

During the past few years methane has often been seen as an alternative source to produce valuable chemicals and H_2. But it is a very stable organic molecule, and new approaches for effective activation for profitable utilization of methane are needed. Mo/ZSM-5 catalysts provide high activities in methane dehydroaromatization (DHA) which is a new way of direct methane conversion. It is shown [1] that steam-dealuminated Mo/ZSM-5 has a much higher selectivity towards aromatics compared with conventional catalysts. There are also many studies assuming that the framework aluminum is easily extracted by the introduction of molybdenum species [2]. On the other hand, it is well known the dealumination treatment of HY zeolite [3] or zeolite BEA [4] leads to creation of a secondary mesoporous system in these zeolites which provides space for the reactions of large molecules [5]. In this study, our goal was to determine the structural changes of Mo/ZSM-5 catalysts during the DHA of CH_4 and following oxidative treatment.

For this we investigated the effect of Si/Al ratio of parent H-ZSM-5 zeolite and molybdenum content on structural changes of Mo/ZSM-5 catalysts during the DHA reaction and subsequent regeneration, using X-ray powder diffractometry, N_2 adsorption and transmission electron microscopy.

Experimental

Catalyst preparation

H-ZSM-5 zeolites with Si/Al atomic ratios 17, 30, 45 were used to prepare Mo/ZSM-5 catalysts. Their main characteristics are presented in [6]. Zeolites with Si/Al = 17 were used in all experiments where the atomic Si/Al ratio is not mentioned specifically.

Samples of Mo/ZSM-5 with molybdenum content of 2 and 10 wt. % were prepared via incipient wetness impregnation of zeolites with ammonium heptamolybdate ($(NH_4)_6Mo_7O_{24}*4H_2O$, "chemically pure" grade) solutions of different concentrations. The prepared samples were dried

*corresponding author. E-mail: zri@catalysis.ru

Printed in Kazakhstan

and calcined at 500°C for 4 h. The Mo/ZSM-5 catalysts before reaction were denoted as parent catalysts.

Catalyst characterization

The chemical composition of the parent zeolites and molybdenum content in the prepared catalysts were determined by means of inductively coupled plasma atomic emission spectroscopy (ICP-AES).

X-ray powder diffraction (XRD) patterns were obtained using the model HZG-4C (Freiberger Prazisionmechanik) diffractometer using CuK_α radiation, over a 2θ range of 5^o-50^o.

Micropore and external surface areas, micropore and mesopore volumes of the parent zeolite and Mo/ZSM-5 catalysts were studied in a Micromeritics ASAP 2400 instrument using *N_2 adsorption at 77 K*. The total surface areas were calculated by the BET method. The external surface area and micropore volume were calculated using the t-plot method. The pore size distribution profile was calculated by using the BJH method applied to both the N_2 adsorption and desorption branches of isotherm.

Transmission electron microscopy (TEM) images were obtained using a JEOL Model JEM-2010 electron microscope with accelerating voltage 200 kV and lattice resolution 0.14 nm. The samples were deposited on perforated carbon supports that were attached to the copper grids. The local elemental analysis of the samples was performed by an EDX method, using an EDAX spectrometer equipped with a Si (Li) detector which had an energy resolution of 130 eV.

Catalytic activity measurement

The catalytic activity of Mo/ZSM-5 catalysts in DHA of CH_4 was measured at atmospheric pressure in a flow setup with a quartz reactor (9 mm inner diameter) as described in detail elsewhere [6]. The catalyst loading was 0.6 g (~ 1 cm^3); 0.25-0.5 mm catalyst fraction was used. Before the reaction the catalyst was heated in argon flow at a flow rate of 30 ml/min to 720°C, with a heating rate 10°C/min, and maintained at this temperature for 60 min. The feed then was switched to the initial reaction mixture, which consisted of 90 vol.% CH_4 and 10 vol.% Ar at a flow rate 13.5 ml/min. The Mo/ZSM-5 catalysts after 6 h reaction were denoted as used catalysts.

The oxidative treatment (regeneration) of the used Mo/ZSM-5 catalysts was carried out in the same flow setup at oxygen atmosphere at 520^oC. These catalysts were named as regenerated catalysts.

The analysis of the reaction mixture were performed using the online automatic gas chromatography system Kristall-2000M equipped with a flame ionization detector and a thermal conductivity detector [6].

The catalytic activity was characterized by the total methane conversion, %, methane conversion to benzene, %, and selectivity of benzene formation, %.

Results

X-ray powder diffractometry

To investigate the possible structural changes in the used and regenerated Mo/ZSM-5 catalysts X–ray diffractometry was used. According to the XRD data for the parent sample, H-ZSM-5 zeolite phase is the predominant crystal phase both for the used and regenerated Mo/ZSM-5 catalysts with 2 wt. % Mo.

For the parent Mo/ZSM-5 catalyst with 10 wt. % Mo, in addition to H-ZSM-5 zeolite phase the phase of molybdenum oxide MoO_3 (35-609, JCPDS) is detected. The pretreatment of this sample in Ar at 720^oC leads to the formation of a new phase which is observed as halo with a maximum in the 2θ range of 18-28°. It is likely that an intermediate molybdenum oxide phase Mo_9O_{26} (5-337, JCPDS) or Mo_4O_{11} (5-441, JCPDS) phase is formed [7,8]. For the used sample with 10 wt. % Mo, the formation of X-ray amorphous phase is observed in the form of halo with a maximum in the 2θ range 25-26°. This may be connected with the formation of carbonaceous deposits in the course of the reaction [9,10]. In addition, an indistinct maximum in the 2θ ranges 37-42° is detected which can be assigned to the formation of η-MoC (8-384, JCPDS) or η-Mo_3C_2 (42-890, JCPDS) phase. In the regenerated Mo/ZSM-5 catalyst with 10 wt. % Mo, aluminum molybdate ($Al_2(MoO_4)_3$) phase (23-764, JCPDS) is found, while the intensity of the main zeolite lines is considerably lower.

Thus, according to the XRD data, destruction of the zeolite lattice does not occur during the reaction on Mo/ZSM-5 catalyst with 2 wt. % Mo and its subsequent regeneration. The increase of

molybdenum content up to 10 wt. % leads to dealumination of Mo/ZSM-5 sample after regeneration treatment in oxygen.

N_2 adsorption

Table 1 shows the micropore area, external surface area, micropore and mesopore volumes of the studied samples. In all used Mo/ZSM-5 catalysts, the micropore area and volume were decreased in comparison with these values in the parent samples. This effect is most pronounced for the sample with the highest Mo loading (10 wt. %). It was shown that carbonaceous deposits were formed in methane stream [6] which could cause blocking of the pores. Note that for the regenerated Mo/ZSM-5 catalyst with 2 wt. % Mo all values were reduced by 10% in comparison with these values in the parent sample. But the micropore area and pore volume of the regenerated Mo/ZSM-5 catalyst with 10 wt. % Mo were nearly two times less than those for the parent catalyst and two times more than for the used catalyst (Table 1).

Table 1

Texture properties of parent, used and regenerated Mo/ZSM-5 catalysts with 2 and 10 wt. % Mo

Texture parameter	Mo content, wt. %					
	2			10		
	parent	used	regenerated	parent	used	regenerated
Micropore area, m^2/g	321	215	289	224	48	87
External surface area, m^2/g	12	56	20	30	41	11
Micropore volume, mm^3/g	153	101	139	106	23	44
Mesopore volume, mm^3/g	38	78	47	50	70	29

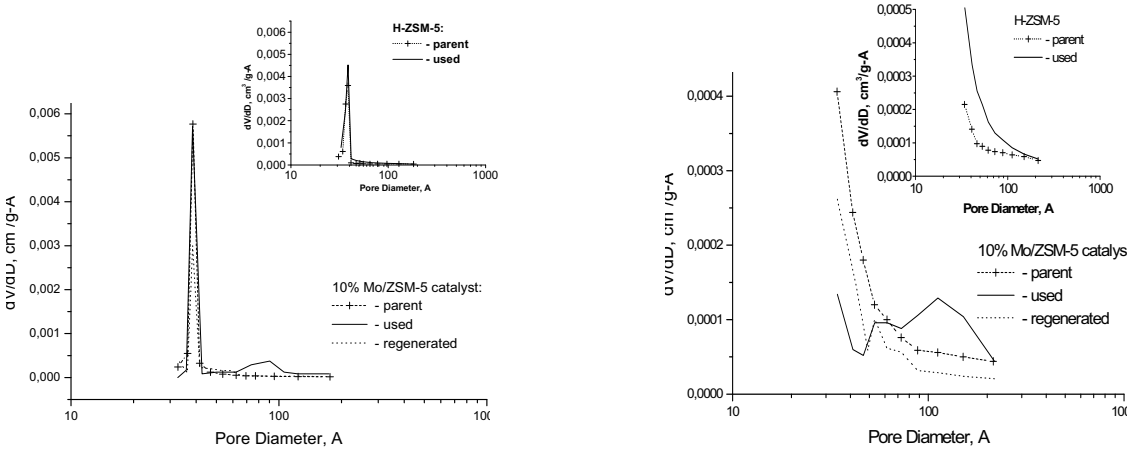

a b

Fig.1. BJH pore size distribution derived from the desorption (a) and adsorption (b) branches of the isotherm of Mo/ZSM-5 catalyst with 10 wt. % Mo. Insets: BJH pore size distribution derived from the desorption (a) and adsorption (b) branch of the isotherm of H-ZSM-5 zeolite.

Differential pore size distribution for H-ZSM-5 and Mo/ZSM-5 catalysts (Fig. 1a) shows a single maximum at 39 Å, which according to [11] does not reflect the exact porous properties of the material but are determined primarily by the nature of absorbate. The additional small maximum appears at 85 Å only for the used Mo/ZSM-5 catalyst with 10 wt. % Mo. But there are no changes in the pore distribution for this regenerated sample in comparison with the parent catalyst.

It was showed [11,12] that the calculation of the pore-size distribution according to the BJH model applied to the adsorption branch of the isotherm was more correct. Differential pore size distribution

for the studied catalyst was calculated in this way too. The results show there are also no differences for the parent, used and regenerated Mo/ZSM-5 catalysts with 2 wt. % Mo. The differential pore size distributions for the used and regenerated Mo/ZSM-5 catalysts with 10 wt. % Mo are the same and have small additional adsorption at 50-100 Å in comparison with the parent catalyst (Fig. 1b). It may be assumed that the mesopore development can cause this new pore size distribution.

So according to N_2 adsorptions, the textural characteristics of Mo/ZSM-5 catalyst with 2 wt. % Mo remain practically unchanged during the reaction and subsequent regeneration treatment. For the catalyst with 10 wt. % Mo, the degradation of the texture occurs and small additional adsorption at 50-100 Å is observed.

TEM

Figures 2 and 3 show the typical TEM images of the Mo/ZSM-5 catalyst with 2 wt. % Mo after pretreatment in Ar at 720°C and used Mo/ZSM-5 catalyst with 2 wt. % Mo, respectively. According to our previous data [6], highly dispersed molybdenum oxide is found on the external surface of the zeolite before the interaction of Mo/ZSM-5 catalysts with methane. Molybdenum carbide particles with sizes of 2-15 nm were found to form on the external surface of the zeolite, and molybdenum-containing clusters with a size about 1 nm were detected in the zeolite channels under the reaction conditions. Two different carbonaceous species were distinguished in addition to the carbidic carbon in molybdenum carbide. The formation of carbonaceous deposits in the form of graphite layers was found on the surface of molybdenum carbide nanoparticles with a sizes of 2-15 nm. At the same time, a friable carbon layer with a disordered structure and inclusions of dispersed graphite with a thickness less than 3 nm were formed on the external zeolite surface of Mo/ZSM-5 catalysts [6].

As apparent from the comparison of Fig. 2 and Fig. 3, aggregation of Mo containing particles occurred and some light streaks appeared in the zeolite grain upon the interaction of methane with Mo/ZSM-5 catalyst with 2 wt. % Mo. It is assumed that pores were formed inside the zeolite crystal of used Mo/ZSM-5 catalyst. The TEM study shows that the pores are open to the exterior of the zeolite grain and have an entrance diameter of ~ 4 nm. The regeneration of the used Mo/ZSM-5 catalyst with 2 wt. % Mo in oxygen leads to the oxidation of molybdenum carbide and desegregation of the particles. As shown in Fig. 4, mesopores in the zeolite grain are also clearly seen in the regenerated Mo/ZSM-5 catalyst. Note that molybdenum oxide particles are concentrated inside the mesopores.

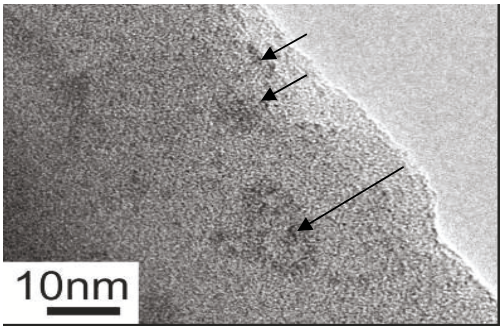

Fig. 2. TEM micrograph [6] of the Mo/ZSM-5 catalyst with 2 wt. % Mo and Si/Al=17 after pretreatment procedures in Ar at 720°C. Surface clusters are shown by arrows.

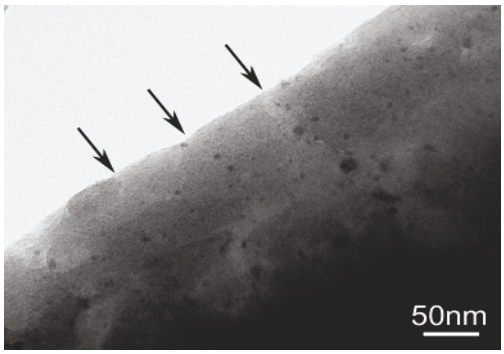

Fig. 3. TEM micrograph [6] of the Mo/ZSM-5 catalyst with 2 wt. % Mo and Si/Al=17 after 6 h on stream in methane dehydroaromatization. The open entrances to mesopores are shown by arrows.

In order to elucidate the influence of the gas medium on the mesoporosity development, the Mo/ZSM-5 catalyst with 2 wt. % Mo was reduced in hydrogen in the flow reactor at 700°C for 1 hour. The light regions with a size of up to 10 nm are observed in the zeolite grains (Fig. 5). It is proposed that mesopores are formed similarly to those in the used and regenerated Mo/ZSM-5 catalysts. There are also many Mo containing particles on the external surface of the zeolite.

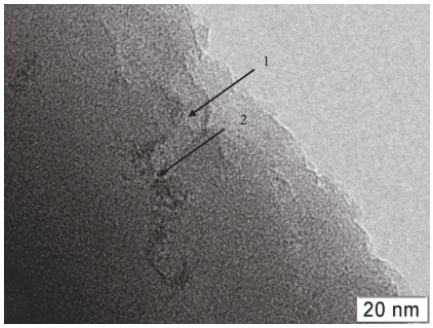

Fig.4. TEM micrograph of the Mo/ZSM-5 catalyst with 2 wt. % Mo and Si/Al=17 after 2 hour of regeneration on oxygen stream at 520°C. The open entrances to mesopores (1) and Mo-containing particles (2) are shown by arrow.

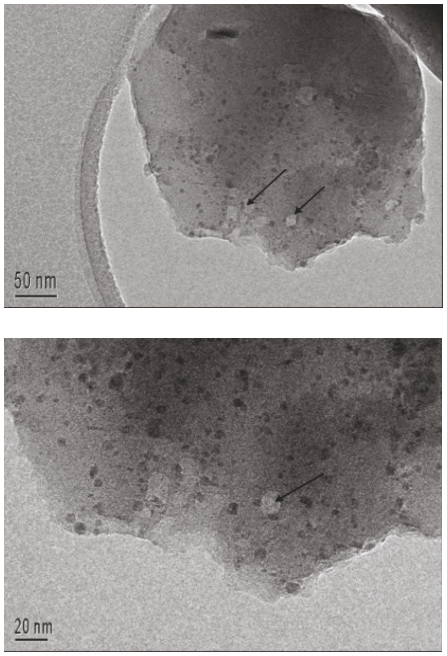

Fig. 5. TEM micrographs of the Mo/ZSM-5 catalyst with 2 wt. % Mo and Si/Al=17 after 1 h on hydrogen stream at 720°C. The mesopore is shown by an arrow.

Fig. 6 shows the TEM image of the Mo/ZSM-5 catalyst with 10 wt. % Mo after pretreatment in Ar at 720°C. As one can see, in contrast to the Mo/ZSM-5 catalyst with 2 wt. % Mo (Fig. 2), there are many particles with a size from 2 to 50 nm on the external surface of the zeolite. The EDX spectrum of such particle shows the atomic ratio Mo/Al=2.6 and Si/Al=1.2 (Fig. 7a). At the same time for the part of the zeolite surface on which the Mo-containing particles with a size above 2 nm are not shown by TEM, the atomic ratio Mo/Al=0.47 and Si/Al=15.2 (Fig. 7b). It is evidence that the enrichment of Mo containing particles by Al occurs.

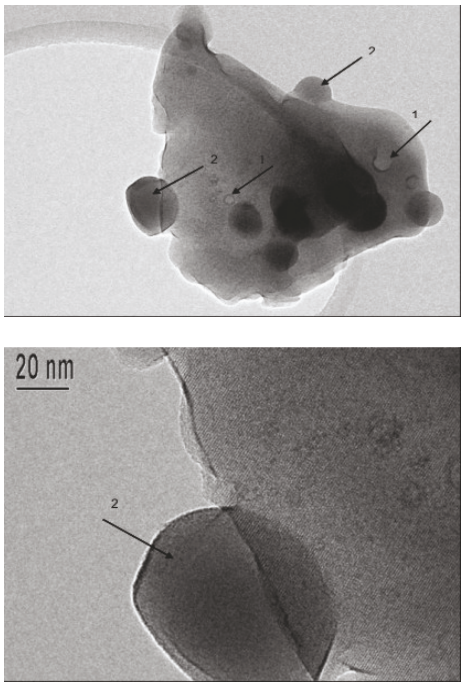

Fig. 6. TEM micrographs of the Mo/ZSM-5 catalyst with 10 wt. % Mo and Si/Al=17 after pretreatment procedures in Ar at 720°C. The mesopores (1) and Mo-containing particles (2) are shown by arrows

In addition, pronounced light regions were observed in the zeolite grain (Fig. 6). Similar TEM image (Fig. 8) is presented for the used Mo/ZSM-5 catalyst with 10 wt. % Mo. The TEM measurement shows that the pores have a diameter about ~ 10 nm.

To determine the influence of Si/Al ratio in zeolites on structural changes of Mo/ZSM-5 samples, the catalysts with 2 wt. % Mo with Si/Al=30 and 45 after 6 h in methane stream were studied by TEM. The TEM measurement shows (Fig. 8a and 8b) that there are mesopores formed in the both samples.

The treatment of the H-ZSM-5 zeolite under similar conditions does not result in the appearance of mesopores. These results led us to conclude that the creation of mesopores in Mo/ZSM-5 catalysts was connected with the presence of molybdenum in the zeolite. For Mo/ZSM-5 catalyst with 2 wt. % Mo the formation of mesopores took place not in Ar but in reducing atmosphere (H_2 or CH_4). For Mo/ZSM-5 catalyst with 10 wt. % Mo, mesopores

were observed by TEM both after Ar and CH_4 treatments.

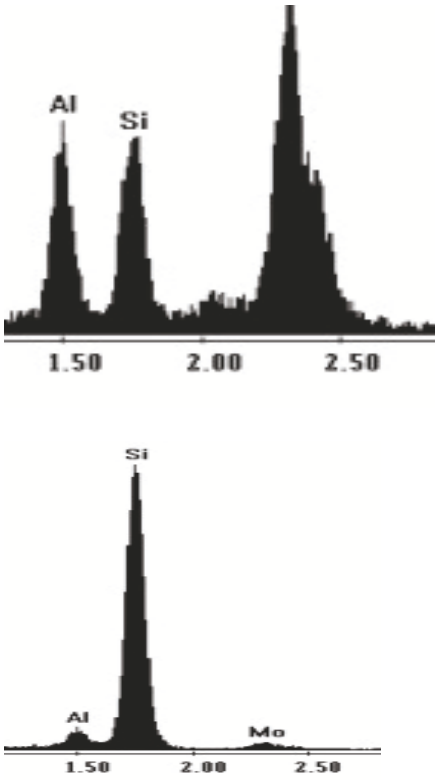

Fig.7. EDX spectra of Mo/ZSM-5 catalyst with 10 wt. % Mo and Si/Al=17 after pretreatment procedures in Ar at 720°C.
(a) – from a Mo-containing particle with size around 50 nm.
(b) – from part of zeolite surface on which the Mo-containing particles with sizes above 2 nm are not shown by TEM

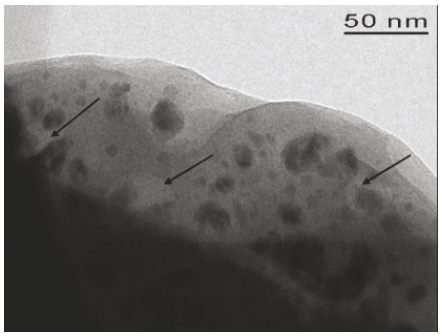

Fig. 8. TEM micrographs of the Mo/ZSM-5 catalyst with 10 wt. % Mo and Si/Al=17 after 6 h on stream in methane dehydroaromatization. The mesopores are shown by arrows.

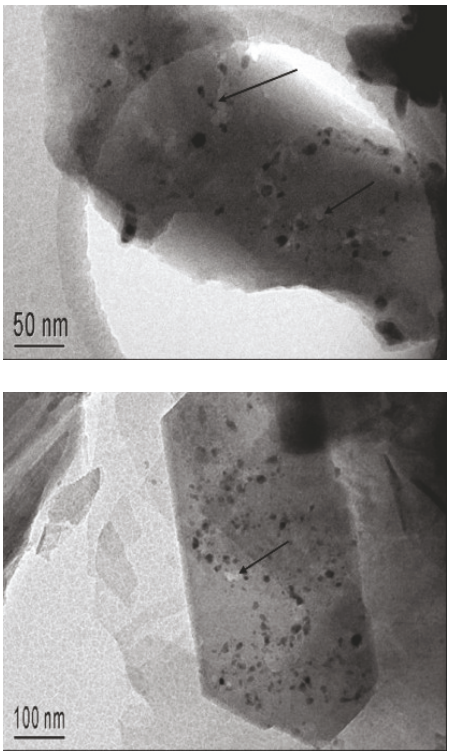

Fig. 9. TEM micrographs of the Mo/ZSM-5 catalyst with 2 wt. % Mo and Si/Al=30 (a) and 45 (b) after 6 h on stream in methane dehydroaromatization. A mesopore is shown by an arrow.

Catalytic activity

To understand how the mesopore formation influences the catalytic activity, the H-ZSM-5 zeolite was treated by NaOH according to the method described in detail in [12]. It was shown [5, 12] that such treatment led to mesopore formation in the zeolite. Indeed, in our case the mesopore surface area increases from 20 to 100 m^2/g and the micropore volume decreases by ~ 20 %, which is in good agreement with [12] and confirms the mesopore formation in the zeolite.

Figure 10 shows the activity of the Mo/ZSM-5 catalysts with 2 wt. % Mo obtained on basis of the parent zeolite and the zeolite treated by NaOH. One can see that the total methane conversion and methane conversion to benzene are higher for the catalyst obtained on the basis of the zeolite without NaOH treatment. The benzene selectivity is the same for the both samples. Thus, mesopore formation in H-ZSM-5 does not improve catalytic activity of Mo/ZSM-5 catalysts.

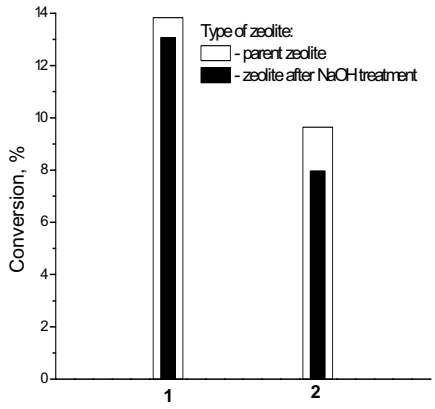

Fig. 10. Total methane conversion (1) and methane conversion to benzene (2) in methane dehydroaromatization on Mo/ZSM-5 catalysts with 2 wt. % Mo and Si/Al = 17 obtained on the basis of the parent zeolite and the zeolite treated by NaOH. Reaction time is 120 min.

Discussion

The results of TEM measurements of the used and regenerated Mo/ZSM-5 catalysts show that the mesopores are formed upon methane dehydroaromatization. Their volume is probably too small to have a strong influence on the N_2 adsorption data and XRD measurement. This brings up the question what is the mechanism of mesopores formation and their effect on the catalytic activity.

As was mentioned above, the formation of mesopores has been reported for H-ZSM-5 zeolites upon alkaline treatment in NaOH solution [5,12] or heat treatment at 950-1100°C [13] for BEA zeolite upon dealumination by hydrothermal treatment and leaching with HNO_3 [4], for Y zeolite upon dealumination in an acidic medium [3]. The development of the secondary porous system was related to the presence of defects in the structure of zeolite crystallites with removed Al or Si atoms. It was shown [3, 5] that the creation of mesopores gave the advantage for the diffusion of reactants and, accordingly, for the accessibility to catalytically active acid sites. Besides, it was noted [2] that the extraction of Al ions from the framework of H-ZSM-5 by Mo species occurred and increased with increasing Mo loading.

So we can assume that the mesoporosity development in Mo/ZSM-5 catalysts during the methane dehydroaromatization is connected with the dealumination of Mo/ZSM-5 catalysts. This assumption is supported by our early ESR data [14], which showed strong interaction between Mo and Al atoms in the Mo/ZSM-5 catalysts during methane dehydroaromatization. Besides, as was noted above, the Mo containing particles are enriched by Al (Fig. 7a).

Thus, the process of structural changes of Mo/ZSM-5 catalysts during the methane dehydroaromatization can be presented in the following way. At first, before the interaction of Mo/ZSM-5 catalysts with methane, the molybdenum in oxygen surrounding is in highly dispersed form both on the external surface and in the zeolite channels. In the reducing atmosphere, Mo particles are aggregated and convert to Mo_2C on the external zeolite surface and to Mo containing clusters in the zeolite channels [6]. Besides, Mo has tendency to react with the framework Al and form Mo-Al clusters which are difficult to reduce in methane at ~ 700°C, such as aluminum molybdate ($Al_2(MoO_4)_3$) both bulk [15] and dispersed on the zeolite surface [16]. This interaction between Mo and the framework Al leads to the zeolite dealumination. The dealumination initiates mesoporosity development, as the linkage of the dealuminated sites, decreasing the strain caused by structure defects [17].

As was showed above, the NaOH treatment of H-ZSM-5 zeolite prior to its impregnation with ammonium heptamolybdate does not improve the activity of Mo/ZSM-5 catalysts.

Conclusions

The changes in the structure of Mo/ZSM-5 catalysts with different Mo content (2 and 10 wt. % Mo) and Si/Al atomic ratio (17, 30, 45) of the parent H-ZSM-5 zeolite during methane dehydroaromatization were studied using X-ray powder diffractometry, N_2 adsorption and transmission electron microscopy.

As determined by XRD, the destruction of the zeolite lattice does not occur during the reaction on Mo/ZSM-5 catalyst with 2 wt. % Mo and its subsequent regeneration. The increase of molybdenum content up to 10 wt. % leads to the dealumination of the Mo/ZSM-5 sample after regeneration treatment in oxygen.

According to N_2 adsorption, the textural characteristics of the Mo/ZSM-5 catalyst with 2 wt. % Mo remain practically unchanged during the

reaction and following regeneration treatment. For the catalyst with 10 wt. % Mo, the degradation of the texture occurs and small additional adsorption at 50-100 Å is observed.

Using TEM, it was shown that during the reaction, the formation of mesopores in the Mo/ZSM-5 catalysts takes place. The pores are open to the exterior of the zeolite grain and have an entrance diameter of ~ 4–10 nm. The capability for mesoporosity development depends on the gas atmosphere and molybdenum content in H-ZSM-5 zeolite. The reducing medium and high molybdenum content in catalysts promote the formation of the mesopores.

It is proposed that mesopore formation in Mo/ZSM-5 catalysts is connected with the zeolite dealumination. The mesopore formation in H-ZSM-5 zeolite by NaOH treatment does not improve catalytic activity of Mo/ZSM-5 in methane dehydroaromatization.

Acknowledgements

Support by the State Contract No 02.513.11.3484 is gratefully acknowledged.

References

1. Lu Y., Ma D., Xu Z., Tian Z., Bao X., Lin L., *Chem. Comm.* 2048 (2001).
2. Liu W., Xu Y., Wong S.-T., Wang L., Qiu J., Yang N., *J. Mol. Catal.* 120:257 (1997).
3. Sasaki Y., Suzuki T., Takamura Y., Saji A., Saka H., J. *Catal.* 178:94 (1998).
4. Bernasconi S., Bokhoven J.A., Krumeich F., Pirngruber G.D., Prins R., *Micropor. Mesopor. Mater*. 66:21 (2003).
5. Ogura M., Shinomiya S., Tateno J., Nara Y., Nomura N., Kikuchi E., Matsukata M., *Appl. Catal. A* 219:33 (2001).
6. Matus E.V., Ismagilov I.Z., Sukhova O.B., Zaikovskii V.I., Tsikoza L.T., Ismagilov Z.R., Moulijn J.A., *Ind. Eng. Chem. Res.* 46:4063 (2007).
7. Bouchy C., Schmidt I., Anderson J.R., Jacobsen C.J.H., Derouane E.G., Derouane-Abt Hamid S.B., *J. Mol. Catal. A* 163:283 (2000).
8. Choi J-S., Bugli G., Djéga-Mariadassou G., *J. Catal.* 193:238 (2000).
9. Irusta S., Cornaglia L.M. and Lombardo E.A., *J. Catal.* 210 (2002) 263.
10. Jóźwiak W.K., Nowosielska M., Rynkowski J., *Appl. Catal. A* 280:233 (2005).
11. Groen J.C., Peffer L.A.A., Perez-Ramirez J., *Micropor. Mesopor. Mater.* 60:1 (2003).
12. Groen J.C., Peffer L.A.A., Moulijn J.A., Perez-Ramirez J., *Col. Surf. A* 241:53 (2004).
13. Zhang C., Liu Q., Xu Z., Wan K., *Micropor. Mesopor. Mater.* 62:157 (2003).
14. Vasenin N.T., Anufrienko V.F., Ismagilov I.Z., Larina T.V., Paukshtis E.A., Matus E.V., Tsikoza L.T., Kerzhentsev M.A., Ismagilov Z.R., *Topics Catal.* 32:61 (2005).
15. Xu Y., Liu W., Wong S.-T., Wang L., Guo X., *Catal. Lett.* 40:207 (1996).
16. Kim Y.-H., Borry R.W., Iglesia E., *Micropor. Mesopor. Mater.* 35-36:495 (2000).
17. Sato K., Nishimura Y., Matsubayashi N., Imamura M., Shimada H., *Micropor. Mesopor. Mater.* 59:133 (2003).

Received 8 iune 2009.